CIRUGIA Y CIRUJANOS
ISSN / eISSN 0009-7411
Publisher MEXICAN ACAD SURGERY,
CENTRO MED NAC SIGLO XXI, EDIFICIO BLOQUE B,
SOTANO, AVE CUAUHTEMOC NO 330,
MEXICO D G, MEXICO, 06700
Volume 26-Issue 1-(2026)
DOI:http://doi.org/10.65281/706343

4D-Based Quantitative Proteomics Reveals Brain Protein Profile Alterations in Mice with arsenic-induced reduced tolerance to acute cerebral ischemia in mice

Yinglu Liu[a]*, Yanhui Li[a], Hu Fang[a], Liangju Sun[a]

[a] Key Laboratory of Environmental Pollution Monitoring and Disease Control, Ministry of Education, School of Public Health, Guizhou Medical University, Guiyang 561113, China

1. Introduction

Arsenic, as a natural element that is present in both inorganic and organic forms in the environment, is a highly toxic metalloid element affecting thousands of people around the world from drinking water or contamination from the leaching of mine deposits and emissions from industries[1]. Arsenicosis has been observed in many American and Asian countries, including Chile, Bangladesh, India, and China[2]. Chronic exposure to arsenic via drinking water and food has emerged as a public health concern worldwide. Many adverse health effects including skin diseases (i.e., arsenicosis, hyperkeratosis, pigmentation changes), carcinogenesis, cardiovascular diseases, and cerebrovascular and neurological diseases have been reported due to arsenic exposure[3, 4].

In numerous cardiovascular and cerebrovascular related studies, cerebral ischemia tolerance has received more and more attention due to its prominent protective effect in cerebral ischemia. Ischemic tolerance is an endogenous protective mechanism induced by nonischemic PC such as hypoxia(Gidday et al., 1994), as well as other physical, chemical, or pharmacological treatments (termed cross tolerance). The protective effect of enhanced tissue ischemia tolerance has been observed in many organs, including the heart[5], liver[6], kidney[7], skeletal muscle[8], and the brain[9, 10], which is the organ most vulnerable to ischemia[11]. Therefore, the study of cerebral ischemia tolerance has become an indispensable part of the research team of cerebral ischemia prevention and treatment.

There is substantial evidence that long-term chronic exposure to arsenic can increase the risk of cardiovascular and nervous system diseases[12-14]. However, due to the lack of evidence linking total arsenic or total inorganic arsenic exposure to the incidence of

ischemic stroke, the effect of arsenic exposure on the incidence of ischemic stroke has been considered nonexistent or negligible for a long time. Until recent years, some studies have shown that arsenic in drinking water even at low concentration is associated with higher incidence rate of stroke[15], and the content of some metabolites of inorganic arsenic in urine is positively correlated with the incidence of ischemic stroke[16]. In addition, arsenic exposure can induce cerebrovascular diseases and increase the risk of atherosclerotic diseases, thus participating in the occurrence and development of cerebrovascular diseases. As a result, the association between arsenic exposure and the onset of ischemic stroke has also received renewed attention. In addition, arsenic exposure can also affect the nervous system at the cellular level, significantly affecting the form and function of neurons, microglia, astrocytes, endothelial cells and other functional cells of the nervous system, which may also affect the occurrence and development of the pathological process of ischemic stroke. The reason is that the relationship between arsenic exposure and arsenic methylation on the incidence of ischemic stroke may be related to the potential effects of inducing inflammation and oxidative stress in the body. In conclusion, the research on the potential role of long-term arsenic exposure and arsenic methylation in the pathogenesis of stroke is of great significance for the prevention and treatment of cerebrovascular diseases in the future.

Therefore, in this study, the effects of arsenic on cerebral ischemia tolerance of mice exposed to arsenic in drinking water were investigated and protein molecules that might play a role were screened out through the detection of cerebral ischemia tolerance and the analysis of brain tissue proteomics.

2. Materials and methods

2.1 Chemicals

Sodium arsenite was obtained from Sigma-Aldrich (USA).

2.2 Experimental animals and treatments

Six-week-old male and female pathogen-free adult male C57BL/6 J mice (18-22g) were obtained from Center for Experimental Animals at Guizhou Medical University (Guiyang, China) with the National Animal Use License number (SYXK(Gui)2023-

0002)（SYXK(贵)2023-0002）.Mice were maintained in a regulated environment (22±1 °C) with a 12 h: 12 h light: dark cycle, and were fed standard chow diet. All animal studies followed standard settings approved by the Experimental Animal Research Committee of Guizhou Medical University and conformed to internationally accepted ethical standards (Guide for the Care and Use of Laboratory Animals). All efforts were made to minimize the numbers of animals used and ensure minimal suffering.

The mice were divided into two groups with 30 mice per group (15 males and 15 females).

Group 1: Control mice exposed to normal drinking water for 90 days;

Group 2: Mice exposed to 10 mg $NaAsO_2$/L via drinking water for 90 days.

The dose of $NaAsO_2$ was chosen from previously published data[17].Since people of all genders and ages are usually exposed to environmental pollutants for a long time in daily life, combined with the existing studies, the exposure time of the experimental animals used in our study was 90 days[18]. We chose arsenite instead of arsenate because in most of the reported incidences of contaminated water As occurs as arsenite and its oxidation to arsenate is necessary for complete As removal[19].

2.3 Detection of ischemic tolerance in mice

After 90 days of arsenic exposure to drinking water, acute permanent global cerebral ischemia models of mice in the blank group and the arsenic exposure group were prepared by two-vessel occlusion (2VO) method[20, 21]. Surgery for 2VO was performed at normal temperature and pressure. To do this, the isoflurane concentration was increased to 5% for 2 min, and the proximal and cephalic ends of the bilateral common carotid arteries (including the vagus nerve) were ligated with wires respectively, and then cut in the middle. The time from the completion of the operation to the death of each mouse was recorded. Mice that breathe less than five times per minute are considered dead.

2.4 Proteome sample preparation

Samples were taken from the refrigerator at -80℃, ground into powder form in liquid nitrogen and transferred to a centrifuge tube. Then added into the sample protein

cracking solution tube. Protein cracking solution was added into the sample in the centrifuge tube, mixed and incubated on ice for 5 min. Then DTT with a final concentration of 10mM was added and centrifuged at 13000g at 4℃ for 20min after 5-15min of ice bath ultrasound, and the supernatant was transferred to the centrifuge tube. Add cold acetone (4 times the volume of supernatant liquid), stand for 2 hours at -20℃, centrifuge, discard the supernatant, add 1ml cold acetone (including DTT with final concentration of 10mM) into the precipitation, and stand for 30 minutes at -20℃ after vortex oscillation; 13000g centrifuge discard supernatant, air dried protein precipitation; Add 8M urea/100mMTEAB(pH 8.0) solution resoluble protein. Add DTT to the final concentration of 10mM, 56℃ water bath for 30min; Add IAM to the final concentration of 55mM, and leave it at room temperature for 30min away from light. Add 4 times the volume of cold acetone, the final concentration of 10mM DTT, stand for 2h at -20℃; Centrifuge at 4℃13000g for 20min, discard the supernatant, and air dry the protein precipitation.For qualified samples, 100 μg protein was taken from each group, and trypsin was added according to the ratio of trypsin: protein =1:50. After enzymolysis at 37℃ overnight, the desalted peptide segment was vacuum freeze-dried. The peptide lyophilized powder was redissolved in 0.1% formic acid solution at 0.1 μg/μl and stored at -20℃ for liquid chromatography-tandem mass spectrometry (LC-MS/MS) analysis.

2.5 LC-MS/MS analysis

Samples were separated using a NanoElute system with a nanolift flow rate. The mobile phase A consists of 0.1% formic acid aqueous solution and the mobile phase B consists of 0.1% formic acid acetonitrile aqueous solution (acetonitrile is 100%). The samples were fed into IonOpticks (Australia, 25cm×75 μm, C18 packing 1.6 μm) by an automatic samper and separated into analysis columns. The temperature of analysis columns was controlled at 50℃ by an integrated column temperature box. The feeding volume was 200ng, the flow rate was 300nL/min, and the gradient was 60min. The gradient of liquid phase at 60min is 0min-45min, and the gradient of liquid B is 2%-22%. At 45min to 50min, the linear gradient of liquid B is from 22%-35%; In 50min-55min, the linear gradient of liquid B is from 35%-80%. At 55-60min, liquid B was

maintained at 80%.

After the mixed samples were separated by chromatography, mass spectrum data were collected by ddaPASEF mode of timsTOF Pro2 mass spectrometer, so that a suitable collection window could be established by diaPASEF method. The effective gradient of analysis is 60min, the detection method is positive ion, the scanning range of parent ion is 100-1700m/z, the range of ion mobility 1/K0 is 0.7-1.4Vs/cm2, the accumulation and release time of ion is 100ms, the example utilization rate is nearly 100%, the capillary voltage is 1400v, and the drying gas velocity is 3L/min. Drying temperature 180℃. The parameters of DDA-PASEF acquisition mode are: 10 MS/MS scans (total cycle time is 1.17s), charge range 0-5, dynamic exclusion time 0.4min, ion target strength 10000, ion strength threshold 2500, CID fragmentation energy 42eV, isolation window setting: If it is less than 700Th, it is 2Th. If it is more than 700Th, it is 3Th. Parameters in DiaPASEF collection mode are: The Mass Range is about 400-1200, the mobility Range is 0.7-1.4Vs/cm2, the Mass Width is 25Da, the Mass Overlap is 0.1, and the Mass steps per Cycle is 32. The Number of Mobility Windows is 2, with 64 collection Windows. The average collection period was 1.8s.

2.6 Data Processing and Isobaric Tags for Relative and Absolute Quantification

DIA-NN(v1.8.1) is the database search software used for DIA mass spectrum data in this study. Libraryfree method is used to search the database, and the search parameters are as follows: The database is uniprot-proteome_UP000000589_Mus_musculus.fasta database. DIA-NN (v1.8.1) software was used for qualitative and quantitative analysis of protein from mass spectrum data. After standardized treatment, the mean ratio of repeated quantitative values of each protein in all organisms was used as the difference multiple (FC, Fold Change), and the difference test used the quantitative value of each protein in the two groups of samples for t test. For this study, a high peptide confidence (1% FDR) was selected. the cut-off value of 1.5-fold for up-regulated proteins, and 0.6667-fold for down-regulated proteins, p-value <0.05 , were set as differentially expressed proteins (DEPs). The bioinformatics analysis pipeline, including GO and KEGG enrichment, was performed as previously described [22, 23].

2.7 Bioinformatics Analysis

DEPs were analyzed by GO (gene ontology) annotation, KOG (eukaryotic cluster of orthologous group) functional classification, KEGG (Kyoto Encyclopedia of Genes and Genomes) pathways, and Protein domain[22, 23].

2.8 Western blotting

Total protein was extracted from mouse brain tissues using RIPA lysis buffer containing protease inhibitors. Protein concentrations were determined with a BCA assay kit. Equal amounts of protein (20-30 μg) were separated by 10% SDS-PAGE and then transferred onto PVDF membranes. The membranes were blocked with 5% non-fat milk in TBST for 1 hour at room temperature and subsequently incubated with primary antibodies against CFB (1:1000), C8 (1:1000), C9 (1:1000), and β-actin (1:5000) overnight at 4° C. After washing, the membranes were incubated with HRP-conjugated secondary antibodies for 1 hour at room temperature. Protein bands were visualized using an enhanced chemiluminescence (ECL) detection system. The band intensities were quantified with ImageJ software, and the expression levels of target proteins were normalized to β-actin.

2.109 Statistical analysis

Statistical analysis was carried out with SPSS Version 20.0 (SPSS Software, Chicago, IL, United States). The experimental data is shown as the means±SEM. Single factor analysis of variance (ANOVA) was used to detect the different distribution of various groups. The distribution of biometric values is normalized by logarithmic transformation. The statistically significant level was $p < 0.05$.

3. Results

3.1 The ischemic tolerance of mice was weakened after chronic arsenic exposure

To determine the effects of arsenic exposure on the tolerance to cerebral ischemia, mice in the control group and arsenic exposure group were subjected to bilateral carotid artery ligation to prepare permanent global cerebral ischemia model. In this study, the time from the completion of surgery to the death of mice (ischemic tolerance time) was

used as an indicator to evaluate the ischemic tolerance of mice (Daily water intake and weight changes were shown in **Supplemental Figure 1**). The results showed that the ischemic tolerance time of arsenic-exposed male C57/BL6 mice was significantly reduced, but the time of arsenic-exposed female mice had no significant (**Figure 1**). This suggests that long-term arsenic exposure can reduce ischemia tolerance in mice, and there is a sex difference in this effect.

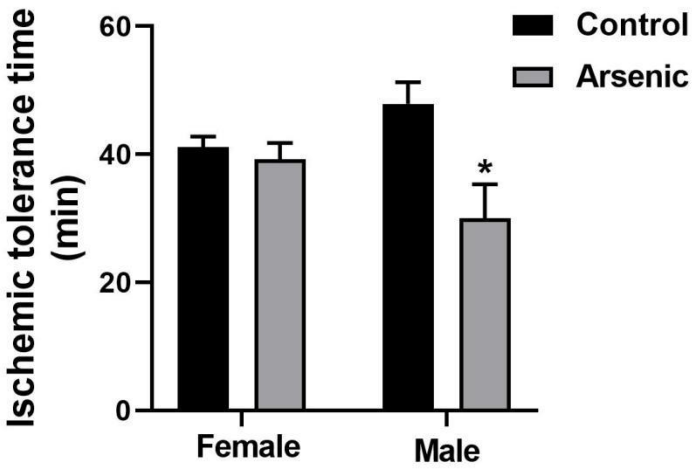

Figure 1

3.2 General Overview of Protein Identification

To explore the protein expression changes during the process of arsenic exposure affecting cerebral ischemia tolerance, 4D-DIA Quantitative proteomics analysis was applied. The results of the quantitative protein principal component analysis for all groups are presented in the below graph (Figure 3). Principal component analysis (PCA) and heatmap clustering enabled a clear discrimination of the protein profiles of the control group and the sodium arsenite exposure group (Fig 3A, B). The intra-group consistency of the samples is good, and the correlation level is high(Fig 3C,D). The total spectrums are displayed in Figure 4B. In total, there are 55,319 available database protein sequences for selection. For the peptides identified, 106529 peptide sequences were resolved via matching; for unique peptides, 106529 peptides were resolved via matching.For identified proteins, 9312 proteins were resolved via unique peptides. For quantifiable proteins, 9312 proteins were resolved via specific peptides.

The ratio of the mean relative quantitative values of each protein in the multiple

replicate samples was used as the fold change (FC) of the difference. To determine the significance of the differences, the relative quantitative values of each protein in the comparison group samples were subjected to a t-test, and the corresponding P-value was calculated as an indicator of significance, with the default being $p < 0.05$. To ensure the test data conformed to the normal distribution required by the t-test, the relative quantitative protein values were log2 transformed prior to the test. With the above analysis of variance, when $p < 0.05$, a change in differential expression of more than 1.3 was used as the threshold of change for significant upregulation, and less than 1/1.3 was the threshold of change for significant downregulation. The differential protein statistics plot (Figure 3F) and the differential protein volcano plot (Figure 3G) show red-colored dots, which represent elevated proteins, and green-colored dots, which represent decreased proteins. The differential protein heat map is presented in Figure 4.

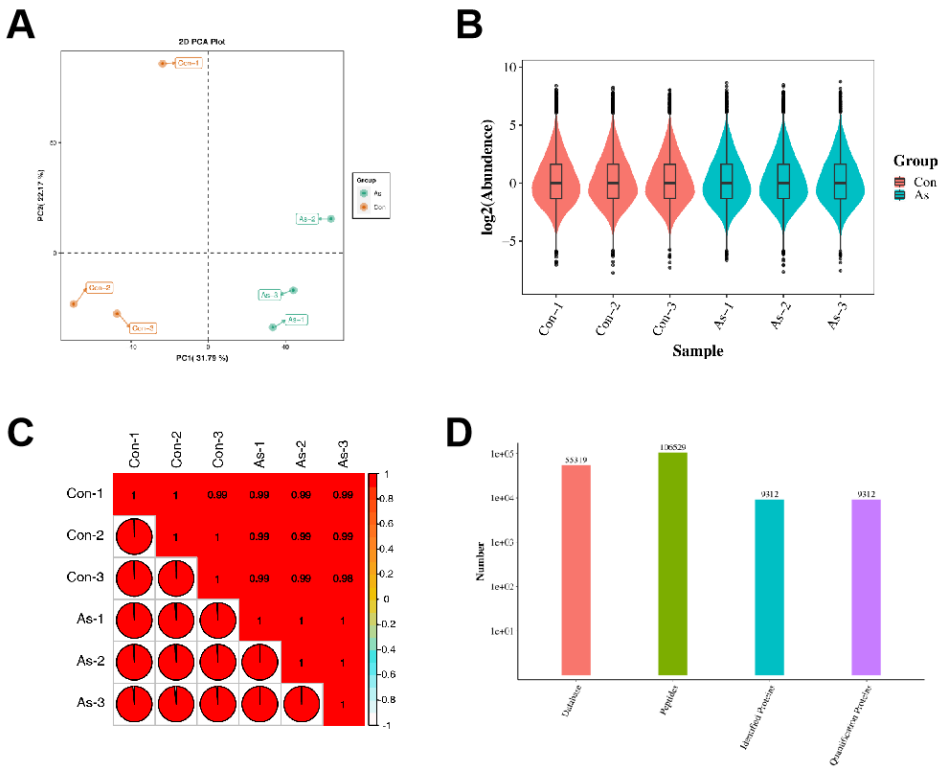

Figure 3. (A) Principal component analysis (PCA) of proteins identified in control group and sodium arsenite exposure group; (B) The distribution of abundance values for the samples in control group and sodium arsenite exposure group; (C) Protein correlation analysis among samples; (D)The results of qualitative and quantitative

analysis of proteins using 4D mass spectrometry data.

A clustering map and volcano plot were further construct to clearly show the differences in protein abundance between the control group and arsenic-exposed group (Figure 4A). A total of 9312 proteins were quantified with a false discovery rate (FDR) <1% (details shown in **Supplemental Table 1**). The results showed that the trend of DEPs exhibited a good consistency between the three samples in each group. According to the following screening criteria of p-value < 0.05 and 1.50-fold change, 51 of the 9312 proteins were regarded as the significant DEPs (Figure 4C). Of these DEPs, 22 were up-regulated proteins, and 29 were down-regulated proteins.

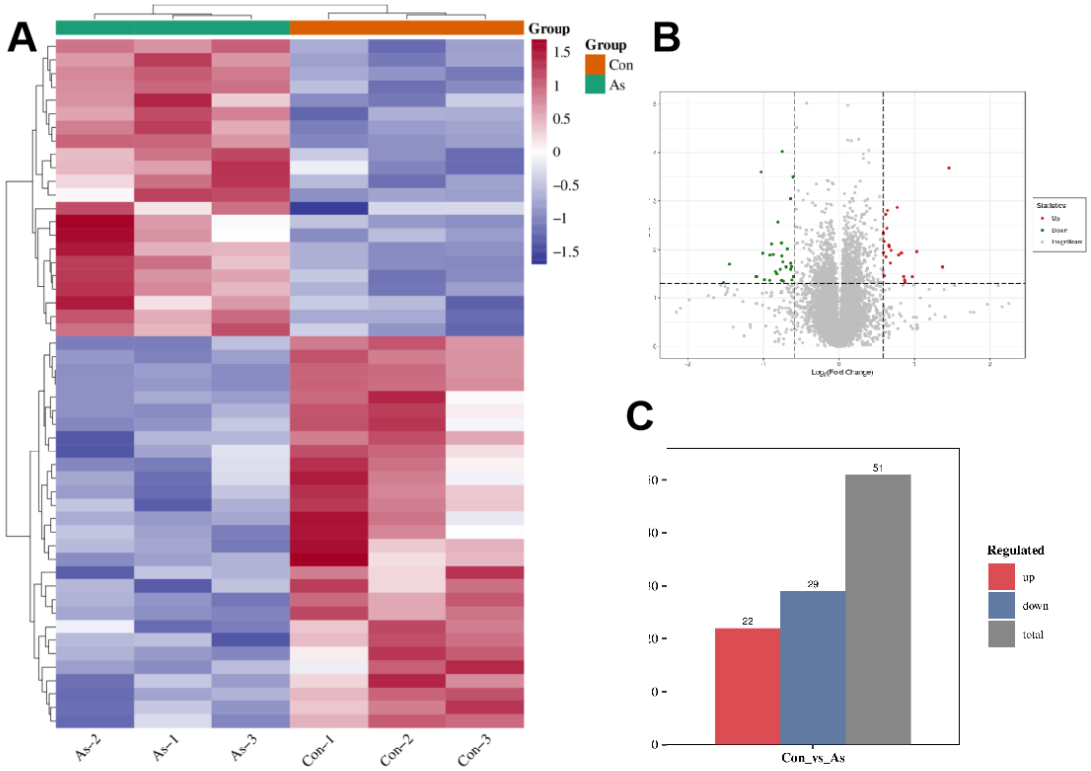

Figure 4. (A) Heat map of protein abundance differences between control group and sodium arsenite exposure group (Red color indicates high abundance, and purple color indicates low abundance); (B)Volcano plot; (C)Statistical results of significantly different proteins.

3.4 GO and KEGG Analysis of Differentially Expressed Proteins

The statistics of differential protein analysis were performed separately for biological processes (BP), cellular components (CC) and molecular functions (MF) (Figure 5A,B). The biological process analysis of the sodium arsenite exposure group/control group was performed first and identified 24 cellular process proteins, 18 regulation of biological process proteins, 15 metabolic process proteins and 10 multicellular organismal process proteins via screening. For cellular fraction analysis, 26 cell-associated proteins, 26 cell part-associated proteins and 18 membrane-associated proteins were screened. In the molecular functional analysis, 26 bindingrelated proteins and 16 catalytic activity-related proteins were observed. Both experimental groups showed greater significant enrichment of ribosomal and ribosomal subunit-related proteins. The analysis of molecular function-related proteins showed significant changes in cell growth factor and energy activity-related proteins in the model group conditions; the enrichment of nucleic acid DNA-related proteins was more significant in the experimental group after dosing compared to the model group. Both experimental groups showed greater significant enrichment of ribosomal and ribosomal subunit-related proteins, and the results are shown in Figure 6C.

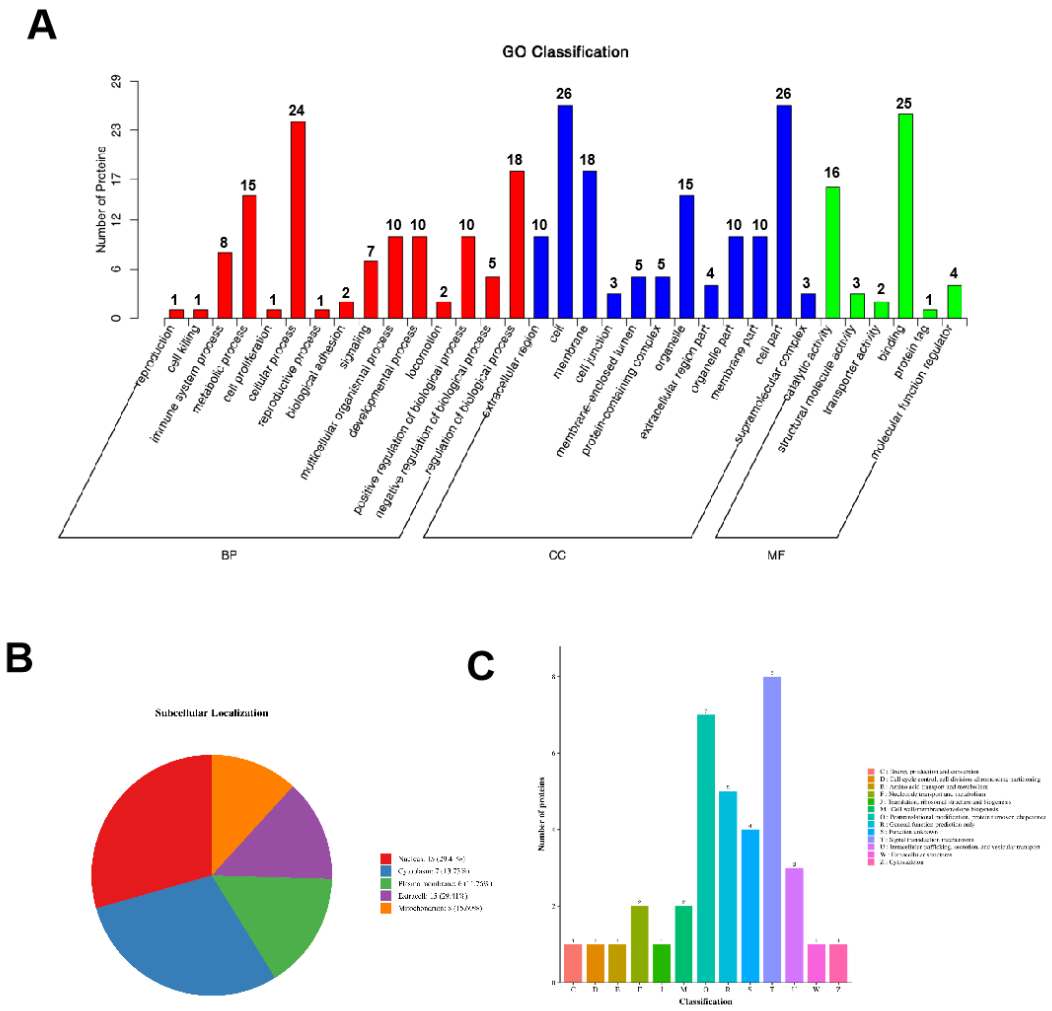

Figure 5. (A) GO secondary annotation classification chart; (B) classification diagram of subcellular structure localization; (C) COG/KOG functional classification chart.

Analysis of the KEGG pathway for all differentially expressed proteins revealed significant changes in the complement and coagulation cascades(**Figure 6**). In the detailed map of this pathway (**Figure 7**). Among the differential proteins identified in this study, complement factor B (CFB), complement component C8 (C8) and complement component C9 (C9) are the most important proteins involved in this pathway.

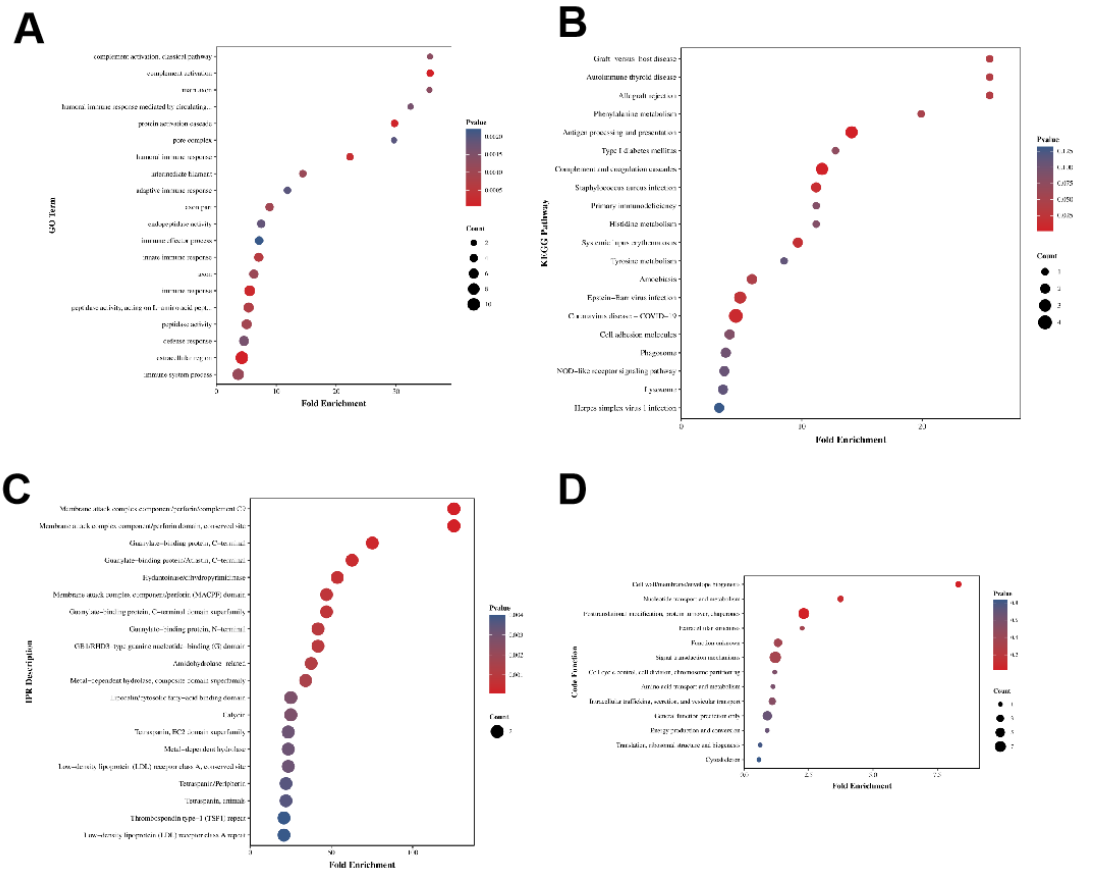

Figure 6 KEGG pathway enrichment analysis of differentially expressed proteins. Bubble plot displays the significantly enriched KEGG pathways ($p < 0.05$) identified from the DEPs between the sodium arsenite exposure group and the control group. The size of the bubble represents the number of proteins enriched in the pathway, and the color indicates the significance level ($-\log_{10}$(p-value)). The complement and coagulation cascades pathway was the most significantly altered, with key DEPs including complement factor B (CFB), complement component C8 (C8), and complement component C9 (C9).

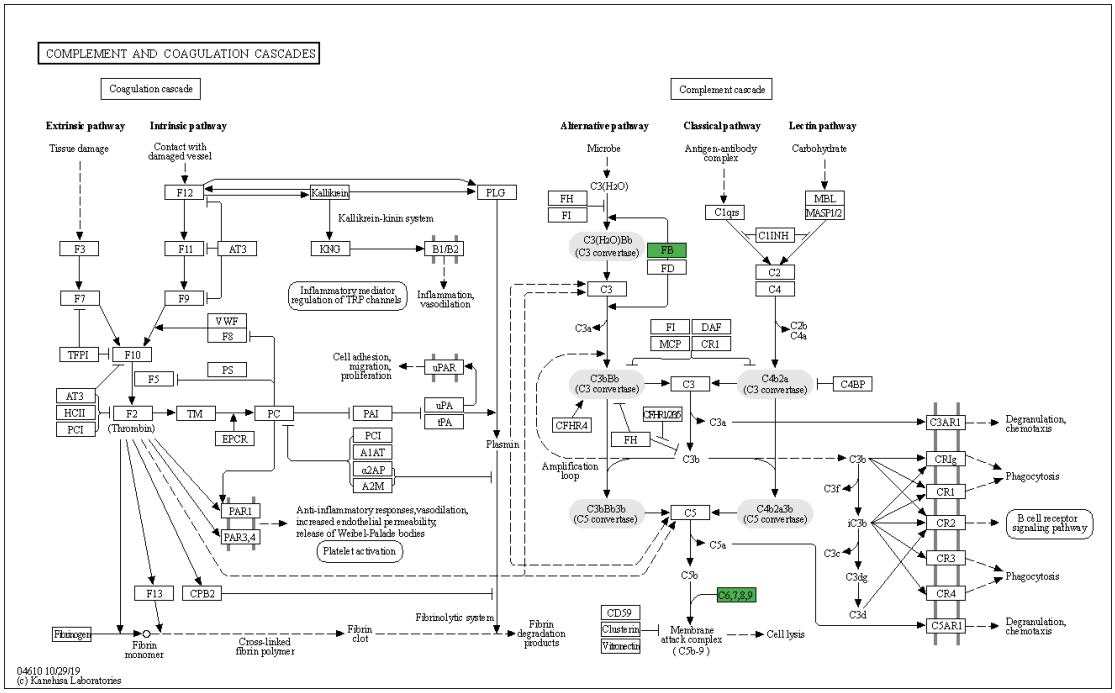

Figure 7 KEGG Complement and coagulation cascades

3.5. Bioinformatics Analysis

3.5.1. Subcellular Structures

The analysis of the main distribution of differential proteins at the subcellular level (shown in Figure 6C, D) was carried out., In the model/control group, 29.41% of the differential proteins were located in the nucleus (Figure 5B), 13.73% were located in the cytoplasm, 11.76% were located in the plasma membrane, 15.69% were located in the mitochondria and 29.41% were located in the extracellular components. A large number of proteins differed between the nucleus, cytoplasm and mitochondria in both groups, suggesting that effects of arsenic on the ischemic tolerance of brain tissue mainly involves mechanisms in the nucleus, cytoplasm and mitochondria.

3.5.2. COG/KOG and Cluster Enrichment Analysis

The COG/KOG functional classification was performed for the differentially expressed proteins listed in Figure 6D. The majority of the differential proteins were signaling proteins, followed by posttranslational modification, protein turnover, chaperones and some proteins with unknown functions were present. The functional categories and pathways in which differentially expressed proteins were significantly enriched ($p <$

0.05) are shown in bubble plots(Figure 6). Cluster analysis was performed to explore the correlation between differentially expressed protein functions in different comparison groups (Figure 8).

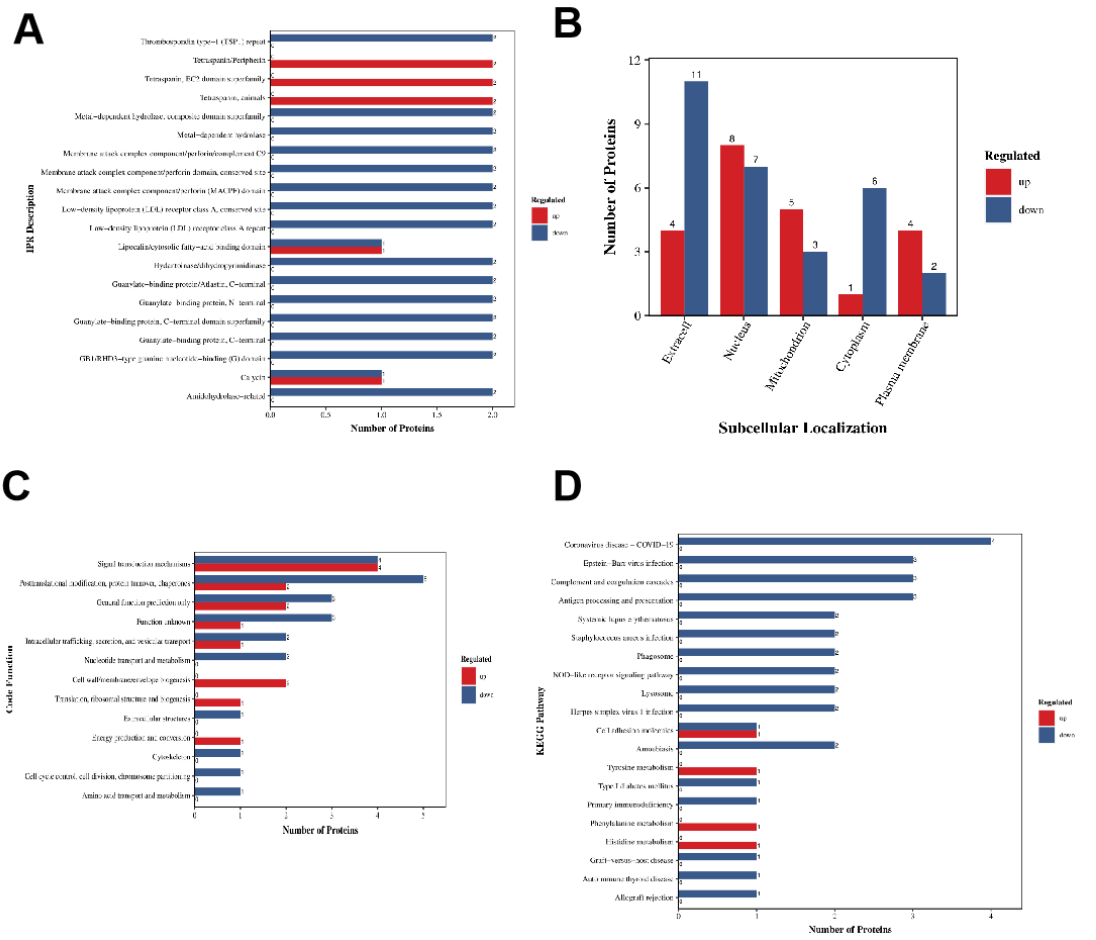

Figure 8. Cluster analysis of differential proteins in up-regulation and down-regulation. (A) Analysis of differentially expressed protein domains; (B)Analysis of the subcellular localization of differential proteins; (C) Analysis of moleculaer function; (D)Analysis of KEGG signaling pathway.

3.6. PPI Analysis

The differential protein interaction network was visualized using Cytoscape 3.8.0 software (Figure 9). Among the proteins that differ significantly in terms of their regulation of cerebral ischemia through complement and coagulation cascades are CFR, C8 and C9. There is a link between the downregulation of CFB and the downregulation of C8 and C9.

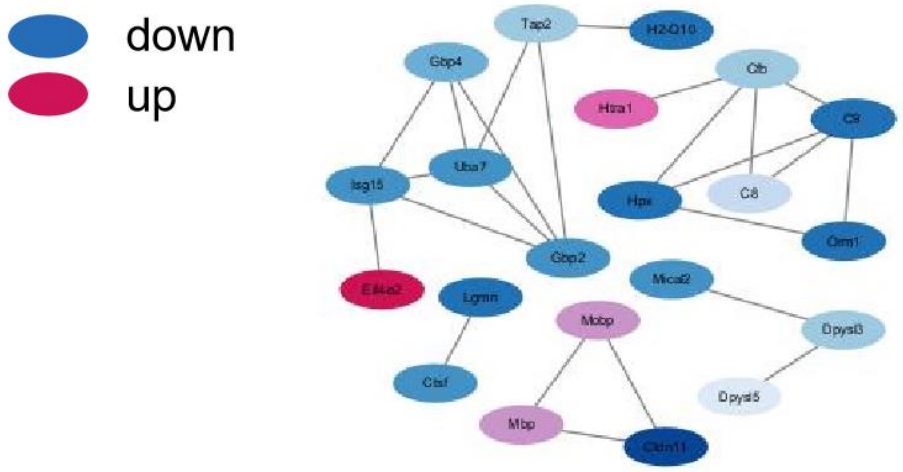

Figure 9 Protein interaction network

3.7. Western Blot Analysis

Compared to the control group, the expression levels of CFR, C8 and C9 in brain were significantly decreased in the model group(Figure 10), which indicates that sodium arsenite exposure can reduce the expression of CFR, C8 and C9 in normal mice, thereby it is possible to influence the ability of mouse brain tissue to tolerate hypoxia by adjusting the complement and coagulation cascades.

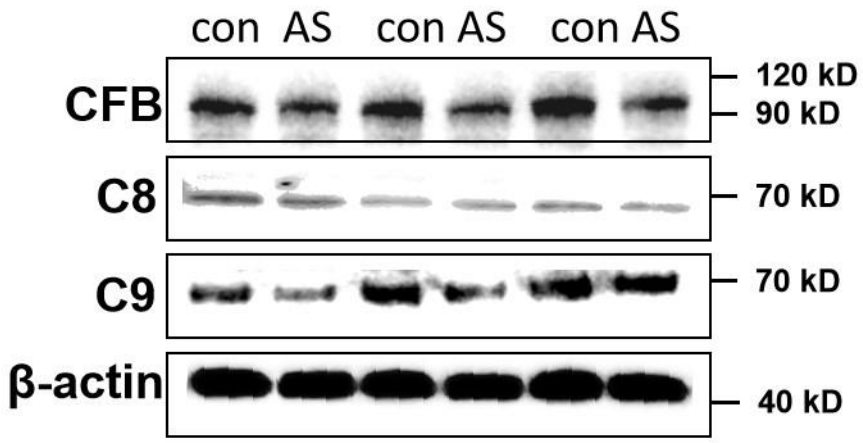

Figure 10. Western blot analysis of CFB, C8, and C9 expression. (A) Representative Western blot images showing the protein levels of complement factor B (CFB), complement component C8 (C8), and complement component C9 (C9) in the control and sodium arsenite exposure (Model) groups. β-actin was used as a loading control. (B) Quantitative analysis of CFB, C8, and C9 protein expression levels normalized to β-actin. Data are presented as mean ± SEM (n = 3-5 per group). *$p < 0.05$ compared to the control group (Student's t-test).

4. Discussion

The findings of this study confirm that chronic arsenic exposure via drinking water reduces cerebral ischemia tolerance in mice, with a significant sex difference—male mice exhibit a marked decrease in ischemic tolerance time, while female mice show no significant change. This sex-specific effect may be linked to differences in arsenic metabolism and detoxification between males and females. Previous studies have indicated that female rodents have more efficient arsenic methylation capacity, producing fewer toxic monomethylarsonous acid (MMAⅢ) metabolites and more non-toxic dimethylarsinic acid (DMAV) metabolites, which could mitigate arsenic-induced neurotoxicity. In contrast, male mice may have lower arsenic methylation efficiency, leading to higher accumulation of toxic metabolites in brain tissue and thus greater impairment of cerebral ischemia tolerance. This is consistent with growing epidemiological evidence linking low-level arsenic exposure to a higher incidence of stroke in human populations [15, 16].

From a proteomic perspective, 4D-DIA quantitative proteomics identified 51 differentially expressed proteins (DEPs) between the arsenic exposure group and the

control group, with 22 up-regulated and 29 down-regulated proteins. GO annotation analysis revealed that these DEPs are mainly involved in cellular processes, biological process regulation, and metabolic processes, and are localized in cell components such as the nucleus, cytoplasm, and mitochondria. This suggests that arsenic exposure may disrupt normal cellular functions in brain tissue, particularly affecting nuclear signaling, cytoplasmic metabolic pathways, and mitochondrial energy metabolism — key processes underlying the maintenance of cerebral ischemia tolerance. Mitochondrial dysfunction, in particular, can lead to reduced ATP production and increased reactive oxygen species (ROS) generation, exacerbating neuronal damage during ischemia and further weakening ischemia tolerance. Arsenic-induced microglia activation and subsequent neuronal damage via inflammatory signaling has been identified as a key mechanism of arsenic neurotoxicity [14].

KEGG pathway analysis highlighted significant enrichment of DEPs in the complement and coagulation cascades, with complement factor B (CFB), complement component C8 (C8), and complement component C9 (C9) being the most critical down-regulated proteins. The complement system plays a dual role in cerebral ischemia: modest activation can clear necrotic cells and promote tissue repair, but excessive activation can trigger inflammatory responses and enhance neuronal injury. In this study, arsenic-induced down-regulation of CFB, C8, and C9 may disrupt the balance of the complement system. During acute cerebral ischemia, insufficient complement activation could impair the clearance of damaged cells, while abnormal complement component expression might also interfere with coagulation function, leading to microcirculatory disorders and reduced blood supply to ischemic brain tissue—both factors contributing to decreased ischemia tolerance. Western blot validation further confirmed the down-regulation of these three proteins, confirming the reliability of the proteomic results and suggesting that the complement and coagulation cascades may be key pathways through which arsenic impairs cerebral ischemia tolerance. The dual role of the complement system in cerebral ischemia, being both protective and detrimental, is an area of active investigation [1, 10].

Notably, the subcellular localization analysis of DEPs showed that a large proportion

of differentially expressed proteins are located in the nucleus and mitochondria. Nuclear proteins are involved in gene transcription and signal regulation, and their abnormal expression may affect the transcription of genes related to ischemia tolerance (e.g., hypoxia-inducible factor HIF-1 α). Mitochondrial proteins, on the other hand, are closely associated with energy metabolism and oxidative stress; arsenic-induced mitochondrial protein dysregulation could disrupt mitochondrial membrane potential, increase ROS production, and trigger neuronal apoptosis, all of which weaken the brain's ability to resist ischemia. The critical role of mitochondrial function and oxidative stress in arsenic-induced toxicity across multiple organs further supports this interpretation [18].

However, this study has certain limitations. First, the mechanism by which arsenic affects the complement and coagulation cascades was not explored at the molecular level (e.g., whether arsenic directly regulates the transcription of CFB, C8, and C9 or affects their expression through intermediate signaling pathways).Future studies should employ integrated multi-omics approaches, as demonstrated in other toxicological models [23], to unravel these complex regulatory networks. Second, the study only observed changes in cerebral ischemia tolerance and protein expression at the endpoint of 90 days of arsenic exposure, lacking dynamic observations at multiple time points, which makes it difficult to clarify the temporal progression of arsenic-induced neurotoxicity. Third, the study did not verify the functional role of key DEPs (e.g., whether overexpression of CFB, C8, or C9 can reverse arsenic-induced reduction in cerebral ischemia tolerance), which needs to be addressed in future studies.

5 Conclusion

This study systematically investigated the effects of chronic arsenic exposure on cerebral ischemia tolerance in mice and the underlying molecular mechanisms using a combination of animal models and 4D-DIA quantitative proteomics. In summary, this study reveals that arsenic exposure impairs cerebral ischemia tolerance in a sex-specific manner by regulating the expression of brain proteins, particularly those involved in the complement and coagulation cascades. These results provide a theoretical basis for the prevention and treatment of cerebrovascular diseases in arsenic-contaminated areas

and offer new insights for further exploring the molecular mechanisms of arsenic neurotoxicity.

Conflicts of interest

The authors declare no conflict of interest.

Acknowledgements

This work was supported by Guizhou Provincial Science and Technology Projects (ZK[2022]371)，National Natural Science Foundation Cultivation Project of Guizhou Medical University (22NSFCP29) and College Students' Innovative Entrepreneurial Training Plan Program(S202310660044)

1. Abdollahzade N, Babri S, Majidinia M: **Attenuation of chronic arsenic neurotoxicity via melatonin in male offspring of maternal rats exposed to arsenic during conception: Involvement of oxidative DNA damage and inflammatory signaling cascades**. *Life sciences* 2021, **266**:118876.
2. Yu G, Sun D, Zheng Y: **Health effects of exposure to natural arsenic in groundwater and coal in China: an overview of occurrence**. *Environmental health perspectives* 2007, **115**(4):636-642.
3. Rahaman MS, Rahman MM, Mise N, Sikder MT, Ichihara G, Uddin MK, Kurasaki M, Ichihara S: **Environmental arsenic exposure and its contribution to human diseases, toxicity mechanism and management**. *Environ Pollut* 2021, **289**.
4. Jia XH, Li YF, Fan YG, Zhou QH, Zhao FH, Qiao YL, Lalley M: **Effect of Arsenic Exposure and Cigarette Smoking on Total and Cause-Specific Mortality: An Occupational Cohort With 27 Follow-up Years**. *Journal of occupational and environmental medicine* 2023, **65**(3):217-223.
5. Murry CE, Jennings RB, Reimer KA: **Preconditioning with ischemia: a delay of lethal cell injury in ischemic myocardium**. *Circulation* 1986, **74**(5):1124-1136.
6. Yadav SS, Sindram D, Perry DK, Clavien PA: **Ischemic preconditioning protects the mouse liver by inhibition of apoptosis through a caspase-dependent pathway**. *Hepatology* 1999, **30**(5):1223-1231.
7. Bonventre JV: **Kidney ischemic preconditioning**. *Current opinion in nephrology and hypertension* 2002, **11**(1):43-48.
8. He W, Zhang J, Zhong A: **[Acute ischemic preconditioning protects against skeletal muscle infarction in the pig]**. *Zhonghua zheng xing shao shang wai ke za zhi = Zhonghua zheng xing*

shao shang waikf [ie waike] zazhi = Chinese journal of plastic surgery and burns 1999, **15**(5):348-350.

9. Weih M, Kallenberg K, Bergk A, Dirnagl U, Harms L, Wernecke KD, Einhaupl KM: **Attenuated stroke severity after prodromal TIA: a role for ischemic tolerance in the brain?** *Stroke* 1999, **30**(9):1851-1854.
10. Kitagawa K, Matsumoto M, Tagaya M, Hata R, Ueda H, Niinobe M, Handa N, Fukunaga R, Kimura K, Mikoshiba K *et al*: **'Ischemic tolerance' phenomenon found in the brain**. *Brain research* 1990, **528**(1):21-24.
11. Hirayama Y, Anzai N, Kinouchi H, Koizumi S: **P2X7 Receptors in Astrocytes: A Switch for Ischemic Tolerance**. *Molecules* 2022, **27**(12).
12. Kuo CC, Balakrishnan P, Gribble MO, Best LG, Goessler W, Umans JG, Navas-Acien A: **The association of arsenic exposure and arsenic metabolism with all-cause, cardiovascular and cancer mortality in the Strong Heart Study**. *Environment international* 2022, **159**:107029.
13. Domingo-Relloso A, Makhani K, Riffo-Campos AL, Tellez-Plaza M, Klein KO, Subedi P, Zhao J, Moon KA, Bozack AK, Haack K *et al*: **Arsenic Exposure, Blood DNA Methylation, and Cardiovascular Disease**. *Circulation research* 2022, **131**(2):e51-e69.
14. Wang H, Chen Y, Liu X, Zhang R, Wang X, Zhang Q, Wei Y, Fang F, Yuan Y, Zhou Q *et al*: **TNF-alpha derived from arsenite-induced microglia activation mediated neuronal necroptosis**. *Ecotoxicology and environmental safety* 2022, **236**:113468.
15. Ersboll AK, Monrad M, Sorensen M, Baastrup R, Hansen B, Bach FW, Tjonneland A, Overvad K, Raaschou-Nielsen O: **Low-level exposure to arsenic in drinking water and incidence rate of stroke: A cohort study in Denmark**. *Environment international* 2018, **120**:72-80.
16. Tsinovoi CL, Xun P, McClure LA, Carioni VMO, Brockman JD, Cai J, Guallar E, Cushman M, Unverzagt FW, Howard VJ *et al*: **Arsenic Exposure in Relation to Ischemic Stroke: The Reasons for Geographic and Racial Differences in Stroke Study**. *Stroke* 2018, **49**(1):19-26.
17. Nordstrom DK: **Public health. Worldwide occurrences of arsenic in ground water**. *Science* 2002, **296**(5576):2143-2145.
18. Li SW, Sun X, He Y, Guo Y, Zhao HJ, Hou ZJ, Xing MW: **Assessment of arsenic trioxide in the heart of Gallus gallus: alterations of oxidative damage parameters, inflammatory cytokines, and cardiac enzymes**. *Environmental science and pollution research international* 2017, **24**(6):5781-5790.
19. Singh R, Singh S, Parihar P, Singh VP, Prasad SM: **Arsenic contamination, consequences and remediation techniques: a review**. *Ecotoxicology and environmental safety* 2015, **112**:247-270.
20. Chen CY, Chen RJ, Lee GA: **Two-vessel Occlusion Mouse Model of Cerebral Ischemia-reperfusion**. *Journal of visualized experiments : JoVE* 2019(145).
21. Pontarelli F, Ofengeim D, Zukin RS, Jonas EA: **Mouse Transient Global Ischemia Two-Vessel Occlusion Model**. *Bio-protocol* 2012, **2**(18).
22. Hu T, Shen L, Huang Q, Wu C, Zhang H, Zeng Q, Wang G, Wei S, Zhang S, Zhang J *et al*: **Protective Effect of Dictyophora Polysaccharides on Sodium Arsenite-Induced Hepatotoxicity: A Proteomics Study**. *Frontiers in pharmacology* 2021, **12**:749035.
23. Zhang D, Wang R, Xiao J, Zhu S, Li X, Han S, Li Z, Zhao Y, Shohag MJI, He Z *et al*: **An integrated physiology, cytology, and proteomics analysis reveals a network of sugarcane protoplast responses to enzymolysis**. *Frontiers in plant science* 2022, **13**:1066073.